

# The relationship between median intensities of electromagnetic emissions in the VLF range and lightning activity

F. Němec<sup>1,2,3</sup>, O. Santolík<sup>2,3</sup>, M. Parrot<sup>1</sup>, C. J. Rodger<sup>4</sup>

---

F. Němec, LPC2E/CNRS, 3A Avenue de la Recherche Scientifique, 45071 Orléans Cedex 2, France.  
(frantisek.nemec@gmail.com)

O. Santolík, IAP/ASCR, Boční II 1401, 14131 Prague 4, Czech Republic. (os@ufa.cas.cz)

M. Parrot, LPC2E/CNRS, 3A Avenue de la Recherche Scientifique, 45071 Orléans Cedex 2, France.  
(mparrot@cns-orleans.fr)

C. J. Rodger, Department of Physics, University of Otago, PO Box 56, Dunedin, New Zealand.  
(crodger@physics.otago.ac.nz)

<sup>1</sup>Laboratoire de Physique et Chimie de  
l'Environnement et de l'Espace / Centre  
National de la Recherche Scientifique, Orléans,  
France.

<sup>2</sup>Institute of Atmospheric Physics, ASCR,  
Prague, Czech Republic.

<sup>3</sup>Faculty of Mathematics and Physics,  
Charles University, Prague, Czech Republic.

**Abstract.** We present results of a survey of VLF electromagnetic waves observed by the DEMETER spacecraft (altitude about 700 km, launched in June, 2004, still operating). The median value of the power spectral density of electric field fluctuations in the frequency range 1–10 kHz is evaluated as a function of the position of the spacecraft, frequency, magnetic local time and season of the year. It is shown that there are significant seasonal differences between the satellite observed wave intensities throughout the year and it is demonstrated that these are due to the lightning activity changes at the Earth. The frequency spectrum at frequencies 0–20 kHz of electromagnetic emissions caused by the lightning activity is investigated as a function of geomagnetic latitude. It is shown that the effect of the lightning activity is most pronounced at frequencies larger than about 2 kHz, forming a continuous band of emissions and being the strongest during the night-time due to the better coupling efficiency of electromagnetic waves through the ionosphere.

---

<sup>4</sup>Department of Physics, University of  
Otago, Dunedin, New Zealand.

## 1. Introduction

Understanding the behavior and properties of electromagnetic waves and their dependence on various parameters is crucial for comprehension of many wave phenomena. Low altitude spacecraft have comparatively short orbital periods and they measure quite often above any given place, it is therefore possible to construct average world maps of electromagnetic emissions. These express the intensity of electromagnetic waves as a function of the spacecraft location (and any other additional parameters, if needed) and they have turned out to be very useful for understanding of the relative importance of various factors that affect wave intensity [Parrot, 1990].

*Koons and Roeder* [1990] presented a survey of wave activity in the equatorial region at radial distances between 5 and 8 Earth's radii. Data from the plasma wave instrument on board the DE-1 satellite have been used to review different types of magnetospheric wave phenomena [Gurnett and Inan, 1988] and, finally, *André et al.* [2002] used DE-1 data to develop an empirical model of low-frequency waves in the plasmasphere.

*Green et al.* [2005] examined data from DE and IMAGE spacecraft, constructed plasma wave intensity maps of whistler mode radiation in the plasmasphere and discussed the occurrence of several main types of waves. Using the data from CRRES spacecraft *Meredith et al.* [2006] concluded that in situ amplification of wave turbulence in space seems to be the main source of wave power below 1 kHz, whereas wave power above 2 kHz is more related to lightning-generated whistlers. Electron loss timescales in the slot region were discussed by *Meredith et al.* [2007, 2009]. They showed that although pitch angle scattering by plasmaspheric hiss is the dominant process responsible for electron loss in the outer slot region ( $2.4 < L < 3.0$ ),

combined effects of hiss and guided whistlers propagating with small wave normal angles are needed to explain the loss timescales at lower  $L$ . All these results strongly suggest the importance of lightning-generated whistlers to the loss of electrons from the radiation belts.

The aim of the present study is to prepare the world maps of electromagnetic emissions at an altitude of 660 km based on about 3.5 years of measurements performed by the DEMETER spacecraft [Berthelier *et al.*, 2006; Parrot *et al.*, 2006]. These maps are then used in order to determine the amount of influence caused by the lightning activity, whose geographical and seasonal dependencies are well known [Christian *et al.*, 2003].

Both the wave and lightning data used in the study are described in Section 2. The obtained results are presented in Section 3 and discussed in Section 4. Finally, Section 5 contains a brief summary of the main results.

## 2. Wave and Lightning Data Used

For this study, we have used the wave data measured by the French micro-satellite DEMETER launched in June, 2004 on a nearly circular orbit. The original altitude (about 710 km) was decreased to about 660 km in December, 2005. Only the data measured at the new satellite altitude have been used in order not to mix the effects from different altitudes. All the data measured up to the end of August, 2009 were used in the study, which represents about 3.5 years of data.

The orbit is quasi Sun-synchronous, which means that DEMETER takes measurements always either shortly before the local noon or shortly before the local midnight. This is demonstrated by Figure 1 that represents the distribution of magnetic local times (MLT) at which DEMETER took the measurements. Two distinct peaks, located approximately at 10.2 MLT

and 22.2 MLT can be clearly seen. These will be referenced to as “day” and “night” in the further text.

The wave instrumentation on board contain both electric field instrument [*Berthelier et al.*, 2006] and magnetic field instrument [*Parrot et al.*, 2006]. Since the magnetic field data can be sometimes disturbed by spacecraft interferences, only electric field data will be used in the presented study. In the VLF range (frequencies up to 20 kHz) this provides us with on-board calculated spectrograms of one electric field component all over the satellite orbit except of the geomagnetic latitudes larger than 65 degrees. The selected electric component is perpendicular to the orbital plane. The frequency resolution of the spectrograms is 19.53 Hz (i. e. 1024 frequency channels ranging from 0 up to 20 kHz) and the time resolution is either 0.512 s or 2.048 s, depending on the sub-mode of the electric field instrument.

Concerning the lightning data, LIS/OTD 2.5 degree Low Res Annual Diurnal Climatology (LRADC) maps have been used [*Christian et al.*, 2003]. This provides us with geographic maps of the lightning activity (i.e. number of lightning strokes per kilometer square per year). For our purposes, these have been recalculated to the corrected geomagnetic coordinates (CGM, see e.g. *Gustafsson et al.* [1992]) and separated using the season of the year and local time [*Rodger et al.*, 2003, 2004, 2005]. Two different seasons have been distinguished: (i) “northern summer”, i. e. May-October and (ii) “northern winter”, i. e. January-April plus November-December. In addition, two different intervals of the local time have been used, corresponding to the local times observed by DEMETER: day-time (8.7–11.7 LT) and night-time (20.7-23.7 LT) – see the dashed lines in Figure 1.

### 3. Results

Figure 2 represents maps in dipole geomagnetic coordinates (resolution  $2.5^\circ \times 2.5^\circ$ ) showing the day-time median value of the power spectral density of the electric field fluctuations in the frequency range 1–10 kHz observed by the DEMETER spacecraft. This frequency range was chosen to correspond to the frequencies most likely affected by the lightning activity: frequencies lower than 1 kHz are unlikely to be affected due to the cut-off frequency of the Earth-ionosphere waveguide [Cummer, 2000] and, on the other hand, data at frequencies larger than 10 kHz may be significantly biased by the signals coming from VLF transmitters [Parrot, 1990]. The top panel was obtained for the period of May-October, i.e. the northern summer. The bottom panel was obtained for the period of January-April and November-December, i.e. the northern winter. The color scale is the same for both panels. The principal advantage of the dipole geomagnetic coordinates as compared to the geographical coordinates is that they enable an easy check for the geomagnetically conjugate regions – these have the same values of the geomagnetic longitude and opposite values of the geomagnetic latitude. Note that the absence of data at large geomagnetic latitudes is caused by the technical limitation of the DEMETER spacecraft (see Section 2). It can be seen that during the period of the northern winter the overall intensity is quite weak and concentrated almost uniformly at larger geomagnetic latitudes. On the contrary, during the period of northern summer two geomagnetically conjugate clearly distinguishable areas of enhanced intensity are formed. They are observed at geomagnetic latitudes larger than about 40 degrees and their geomagnetic longitudes approximately correspond to the geomagnetic longitudes of North America.

Figure 3 uses the same representation and color scale as Figure 2, but it shows the results obtained during the night-time. Here, the situation is a bit more complicated. Similarly to the day-time results, two geomagnetically conjugate areas of enhanced intensity are observed dur-

ing the northern summer at geomagnetic longitudes of North America. The most significant difference as compared to the day-time results is that this time the increase of intensity is enormous, much larger than during the day-time. One can observe other areas of increased wave activity as well, although they are generally less pronounced. For the northern summer the top panel of Figure 3 shows these additional areas of enhanced intensity: (i) equatorial Africa, especially its western part (ii) central Europe and its geomagnetically conjugate region to the South of Africa (iii) all the band within  $\pm 30^\circ$  from the geomagnetic equator starting at the geomagnetic longitudes of India and extending up to the geomagnetic longitudes of Japan. During the northern winter (i.e. the bottom panel of Figure 3), there is no significant increase of intensity at geomagnetic longitudes of America except of a small region of weakly enhanced intensity located to the South-East from North America. However, there are other areas of the increased intensity. The most clearly pronounced area of increased intensity is located above southern Africa and close to the geomagnetically conjugate region. In addition, a zone of increased intensity is also located above northern Australia and its geomagnetically conjugate region. Finally, there is a nearly continuous band of emissions at large geomagnetic latitudes ( $L > 3$ ) observed in the southern hemisphere, spanning from longitudes of Africa up to the longitudes of New Zealand.

In order to explain the existence of these areas of increased power spectral density of electric field fluctuations, we will examine the global distribution of the lightning activity. Figures 4 and 5 represent distributions of the night-time (20.7 – 23.7 LT) lightning activity (resolution  $2.5^\circ \times 2.5^\circ$ ) obtained for the period of northern summer and northern winter, respectively. They are plotted in geomagnetic coordinates and both use the same representation. Since a definition of CGM coordinates at the near-equatorial region is rather problematic [*Gustafsson et al.*,

1992] and our tracing routine used for the conversion of lightning data from geographic to CGM coordinates may produce inaccurate results in this area, any lightnings within  $\pm 5$  degrees of the geomagnetic equator have been removed. The top panel shows the observed number of lightning strokes per square kilometer per year. The two basic well-known phenomena can be seen: (i) lightning occurs more often above the continents than above the oceans; the average land/ocean ratio as reported by *Christian et al.* [2003] is about 10:1 (ii) lightning tends to occur more often during the “local summer” – i.e. during the northern summer they are observed more often in the northern hemisphere and during the northern winter they are observed more often in the southern hemisphere. This crucial difference in the lightning occurrence rate as a function of the position and season of the year enables us to distinguish the effects connected with the lightning activity by studying their geographical and time distribution. This is the approach that will be used in the present study.

The middle panels of Figures 4 and 5 represent the same maps of lightning activity as the top panels, but this time “symmetrized”: the value in each bin is calculated as a sum of the lightning activity in the given region and of the lightning activity in the region which is geomagnetically conjugated. The reason for this procedure is that the electromagnetic waves that we are interested in are believed to propagate in the whistler mode along the magnetic field lines and their intensity in geomagnetically conjugate regions is thus connected. This is well documented by the fact that the areas of enhanced wave intensity in Figure 2 and Figure 3 never exist “alone”, but are always complemented by the geomagnetically conjugate region.

The third panels of Figures 4 and 5 show the projection of the symmetrized lightning activity along the magnetic field lines up to the DEMETER altitude. As compared to the middle panels of the appropriate figures, this results to the “shift towards geomagnetic equator” at lower geo-

magnetic latitudes. At larger geomagnetic latitudes, the difference is not very significant and it disappears at the North and South geomagnetic poles, where it would be equal to zero. The purpose of these recalculated maps of lightning activity is to estimate the parts of the satellite orbits which should be affected by individual regions of heavy lightning activity. The principal idea of this calculation is that the electromagnetic waves generated due to the lightning activity close to the Earth's surface propagate up to the satellite altitudes approximately along the magnetic field line. At middle latitudes this approximation causes only a small error that is contained within a few degrees [*Santolík et al.*, 2009; *Fiser et al.*, 2010]. However, at low latitudes this error would slightly increase. This approximation is very useful for our purposes, because it provides us with an upper estimate of the latitudinal shift caused by the ambient magnetic field. Since the lower estimate is the zero latitudinal shift (corresponding to the propagation “directly upwards” – the results plotted in the middle panels), it enables us to determine the range of the possibly affected areas. Consequently, we are able to determine the affected areas at large geomagnetic latitudes quite precisely, but significant uncertainties remain in the equatorial regions.

We have plotted the same results as those depicted in Figures 4 and 5 also for the day-time (not shown here). It turns out that the global distribution of the lightning activity is about the same as during the night-time, except of the lower occurrence rate. This is expected, because the lightning activity is known to peak at any given location at 17–19 LT, meaning that the DEMETER night-time orbits are quite close to the peak time. On the contrary, DEMETER day-time orbits are at such an early part of the day-time that the lightning activity is rather low.

When one compares the areas of increased power spectral density of electric field fluctuations during the night from the top panel of Figure 3 (the bottom panel of Figure 3) with the corresponding lightning distribution plotted in Figure 4 (Figure 5, respectively), a clear corre-

spondence between the two is found. During the period of northern summer, all the areas of increased electromagnetic activity can be directly linked with the high lightning activity and vice versa. The only exception is the equatorial area of the South America, where a significant lightning activity takes place, but it has no observable impact on the wave intensity observed by DEMETER. This is most probably caused by the inefficient coupling of electromagnetic waves between the Earth's surface and DEMETER altitudes at the given location and will be discussed more in detail in Section 4. Concerning the period of the northern winter, the situation is very similar – there is a good correlation between the intensity of electromagnetic waves observed by DEMETER and lightning activity all over the world except of the equatorial regions and the band of increased wave intensity at large negative geomagnetic latitudes (whose source is very unlikely to be lightning and which is beyond the scope of this paper). No such correspondence can be seen in the day-time electromagnetic data plotted in Figure 2, except of the increased wave intensity above North America and the geomagnetically conjugate region during the period of the northern summer. This striking difference between day-time and night-time data is most probably caused by better efficiency of coupling of electromagnetic waves during the night and it will be discussed more in detail in Section 4.

As it can be seen from the presented results, the wave intensity in the frequency range 1–10 kHz is significantly different during the summer and winter periods. In order to check the frequency spectrum of these differences we have chosen the area where the difference is the most striking – i.e. the area defined by the geomagnetic longitudes of the North America (from  $-60^\circ$  to  $20^\circ$  of geomagnetic longitude). For this area and for all the four possible combinations of day-time/night-time and winter/summer data, we have then plotted the median value of the observed power spectral density of electric field fluctuations as a function of the frequency

of the wave and of the absolute value of the geomagnetic latitude. The frequency resolution 19.53 Hz is given by the technical limitations of electric field instrument (see Section 2) and the latitudinal resolution was set to be  $1^\circ$ . All the frequency range covered by the instrument (0–20 kHz) is analyzed this time – although the effect of lightning strokes is expected to be the strongest in the frequency range 1–10 kHz, the used representation enables us to conveniently study also the effects at lower and larger frequencies. The results obtained for the day time are over-plotted in Figure 6, whereas Figure 7 represents the same results obtained for the night time. The black line plotted in all the panels shows one half of the equatorial electron cyclotron frequency calculated at the given L-value using a dipole magnetic field model. The last panels of Figure 6 and Figure 7 represent the total lightning activity in the selected range of geomagnetic longitudes. Solid red curves correspond to the day-time data, whereas solid blue curves correspond to the night-time data. Dashed lines (shifted slightly towards the geomagnetic equator as compared to the appropriate solid lines) trace the projections along the magnetic field lines up to the spacecraft altitude, corresponding thus to the last panels of Figures 4 and 5.

By comparing the top panels of Figures 6 and 7 (significantly affected by the lightning activity during the northern summer) with the middle ones (influenced by the lightning activity only very weakly during the northern winter), one can reveal the frequency spectrum of the emissions related to lightning. The upper limit of this spectrum is quite well defined by one half of the equatorial electron cyclotron frequency at the given L-value, which is a theoretical limit for the upper frequency of the ducted propagation [Walker, 1993; Clilverd *et al.*, 2008]. Moreover, it can be seen that the additional emissions observed during the northern summer are stronger during the night-time than during the day-time, which is in a good agreement with Figures 2 and 3 as well as with our explanation of lower efficiency of coupling of electromagnetic waves

up to the DEMETER altitude during the day-time. Finally, it should be mentioned that the “horizontal lines” of enhanced intensity observed during the night-time at frequencies larger than about 15 kHz are signatures of VLF transmitters. Their occurrence exclusively during the night-time is consistent with the explanation of lower efficiency of coupling during the day-time (see Section 4) – they are too attenuated during their propagation through the ionosphere to be observed in Figures 6 and 7 (*Gamble et al.* [2008] reported that the typical power levels observed during the day above the NWC transmitter operating at 19.8 kHz are  $\approx 1200$  times lower than during the night). It may also be of some interest that their intensity seems to be enhanced at the same range of geomagnetic latitudes where the lightning-induced electromagnetic emissions are observed.

#### 4. Discussion

All the presented results are based on the electric field data, because these contain much less spacecraft interferences than the magnetic field data. However, since the waves are supposed to propagate in the electromagnetic whistler mode, the power spectral density of electric field fluctuations and power spectral density of magnetic field fluctuations are tied by Maxwell equations via the factor containing the refractive index and wave vector direction. This is in an agreement with similar results obtained for the magnetic field data (not shown) – at least as far as the sole electric/magnetic field component measured enables us to check. We can thus conclude that the analyzed power spectral density of electric field fluctuations determined using only one electric field component represents a sufficient proxy for the intensity of electromagnetic waves.

The fact that the lightning activity varies significantly as a function of the geographic location and season of the year enables us to distinguish its effect on the intensity of electromagnetic waves observed by the DEMETER satellite. In Figures 2, 3, 4 and 5 we study the geographical

distribution of power spectral density of electric field fluctuations and geographical distribution of the lightning activity obtained separately for the two seasons of the year, defined as May-October (northern summer) and January-April plus November-December (northern winter). It should be noted that although the spatial resolution used for both DEMETER and lightning activity data is  $2.5^\circ \times 2.5^\circ$ , transmitter signatures in Figure 7 indicate that a single point source may contribute to the received wave intensity from a significant distance away, which may potentially spread lightning signatures observed in Figures 2 and 3 over a larger area.

The observed agreement between the geographic regions of heavy lightning activity and geographic regions of enhanced wave intensity during the night-time suggests that during the night the lightning activity has a major influence on the observed wave intensity above about 2 kHz all over the world except of the areas very close to the geomagnetic equator. Moreover, the fact that increased wave intensity is usually observed not only directly above the lightning-active region, but comparable levels of wave intensity are observed also above the region geomagnetically conjugated, suggests that on average there is no significant attenuation or amplification of the VLF waves as they propagate in the whistler-mode from one hemisphere to another.

During the day the effect of the lightning activity is much less pronounced, being observable only at large geomagnetic latitudes during the period of northern summer at geomagnetic longitudes of North America. In order to explain this, one needs to take into account the efficiency of coupling of electromagnetic waves through the ionosphere. This efficiency of coupling is significantly larger during the night than during the day because of the lower plasma number density. Moreover, the efficiency of coupling is larger at larger geomagnetic latitudes than in the equatorial region both because of the stronger magnetic field and its larger inclination (see, e.g., *Němec et al.* [2008]). The efficiency of coupling of electromagnetic waves up to the satellite

altitude is thus well consistent with the observed geographic distributions. Moreover, it can naturally explain the lack of correlation between the lightning activity and observed wave intensity during the day as well as in the equatorial regions.

Subsequently, we would like to focus a bit more in detail to the regions close to the geomagnetic equator. Here, the correspondence between the lightning activity and the observed intensity of electromagnetic waves is rather poor even during the night time. For sure, this can be partially attributed to the lower efficiency of coupling due to the weaker and less inclined Earth's magnetic field. In addition, *Cilverd et al.* [2008] noted that field-aligned ducts are too weak to guide whistler mode signals through the plasmasphere for latitudes below  $L = 1.6$  (a geomagnetic latitude of about 37 degrees), which may also influence the coupling of waves from lightning into space. Certainly, our wave power distribution resembles the variation with  $L$  of satellite observed whistler induced electron precipitation events [*Voss et al.*, 1998, Figure 11], with the vast majority of both the wave power and precipitation limited inside the L-shells where ducting is possible. However, there are two more important factors that play role. First, plasma number density in the equatorial region is larger than the plasma number density at larger geomagnetic latitudes [see, e.g., *Parrot et al.*, 2008, Figure 3], which results in a more significant attenuation. Second, due to the significant inclination of ambient magnetic field in the equatorial regions it is difficult to find the regions on the Earth's surface and at the DEMETER altitudes that are projected along the wave ray path. We possess only lower and upper estimates of the geomagnetic latitudes of the DEMETER orbit affected by the lightning activity that takes place at a given point. These are obtained by supposing i) a direct (i.e. perpendicular to the Earth's surface) propagation of the wave up to the DEMETER altitude and ii) a propagation along the magnetic field line. These simple estimates are useful for describing

the real situation – as documented by Figures 4 and 5 – and they enable to easily explain why the lightning activity in the equatorial regions does not affect the wave intensity measured by DEMETER. However, the obtained latitudinal interval is quite large for the areas close to the geomagnetic equator, resulting into significant uncertainties.

The results depicted in Figures 6 and 7 use the fact that the lightning activity is significantly dependent on the season of the year in order to determine what is the amount of lightning contribution to the observed intensity of electromagnetic waves at different frequencies and geomagnetic latitudes. The longitudinal region taken into account was arbitrarily chosen to correspond to the geomagnetic longitudes of the North America, where the summer lightning activity is very heavy and the difference between northern summer and winter season is the most striking. The used representation of the color-coded median value of power spectral density of electric field fluctuations as a function of frequency and geomagnetic latitude enables us a detailed study of the influence of the lightning activity.

In Figure 6 it can be seen that two distinct bands of emissions are observed during the northern summer day-time. The lower band of emissions at frequencies up to about 2 kHz is quite persistent and does not seem to depend much on the season of the year, although lightning generated whistlers can penetrate into the ionosphere also at these frequencies [*Santolík et al.*, 2008, 2009]. Their contribution to the total observed power is therefore relatively small during the day. On the other hand, the upper band of emissions is enormously dependent on the season of the year, meaning that it is formed by the emissions connected to the lightning activity. This upper band of emissions seems to be consistent with seasonal variations of whistler induced electron precipitation predicted by *Rodger et al.* [2004] and experimentally confirmed few years later by *Gemelos et al.* [2009]. During the northern summer, it is clearly distinguishable, spreading

over about 25 degrees of geomagnetic latitude and a large frequency range. However, during the northern winter day-time it practically vanishes. During the night-time (Figure 7), when the efficiency of coupling of electromagnetic waves is larger, the intensity of the frequency band below about 2 kHz does show seasonal dependence, suggesting that lightning generated whistlers effectively penetrate into the ionosphere [Santolík *et al.*, 2008, 2009] and their contribution to the total observed power is significant. The intensity of the upper frequency band above about 2 kHz also significantly increases. It is now observable even during the period of northern winter, although it is very weak. The upper frequency limit of this band seems to be connected to the equatorial electron cyclotron frequency along the magnetic field line, which is a theoretical limit for a ducted propagation. This suggests that the observed waves propagate in a ducted mode along the magnetic field lines. This is in a good agreement with the results obtained by Clilverd *et al.* [2008], who concluded that although the waves in the frequency range 18–25 kHz (i.e. frequencies a bit larger than the ones studied in the present paper) are usually unducted at very low L-shells ( $L < 1.5$ ), at larger L-shells they become highly ducted in the plasmasphere.

The band of emissions caused by the lightning activity is limited by two more characteristic frequencies. First, it does not seem to occur at frequencies lower than about 2 kHz (independently of geomagnetic latitude). This frequency threshold is probably caused by the cut-off frequency of the Earth-ionosphere waveguide [Cummer, 2000], which is about 1.7 kHz and which makes it impossible for low-to-mid intensity whistlers at lower frequencies to be observed by the satellite. Second, the upper frequency of the band decreases close to the geomagnetic equator down to about 5 kHz at geomagnetic latitudes of about 10 degrees. We believe that this upper frequency limit might be connected to the wave penetration up to the DEMETER altitudes. From the last panels of Figures 6 and 7 it can be seen that the distribution of the lightning

activity as a function of the geomagnetic latitude has two distinct peaks, one of them at geomagnetic latitudes about 45 degrees and the other one at geomagnetic latitudes about 20 degrees. However, a comparison with the wave intensity observed by DEMETER (top and middle panels) reveals that the peak close to the geomagnetic equator almost does not contribute to the wave intensity, as it is expected from the above discussion of the efficiency of coupling.

## 5. Conclusions

The results of a study of measured power spectral density of electric field fluctuations observed by the DEMETER satellite (as a proxy for the intensity of electromagnetic waves) are presented. It has been shown that – especially during the night where the penetration of electromagnetic waves through the ionosphere is easier – there is a clear correlation between the lightning activity and the observed intensity of electromagnetic waves. It has been shown that this influence coming from lightning strokes is the most important factor affecting the wave intensity at frequencies larger than about 2 kHz. Moreover, the summer-winter asymmetry in the lightning occurrence rate enabled us to separate the emissions caused by the lightning activity and to check their frequency-geomagnetic latitude dependence. It was shown that the observed emissions are most probably ducted along the magnetic field lines, because they exhibit an upper frequency limit corresponding to one half of the equatorial electron cyclotron frequency at a given L-shell, which is a theoretical limit for a ducted propagation.

**Acknowledgments.** DEMETER is currently operated by CNES and the corresponding staff is deeply acknowledged. We also thank J. J. Berthelier, who is the PI of the electric field instrument. This work was supported by AVCR and by grants GACR 205/09/1253 and ME 09107.

## References

- André, R., F. Lefeuvre, F. Simonet, and U. S. Inan (2002), A first approach to model the low-frequency wave activity in the plasmasphere, *Ann. Geophys.*, *20*, 981–996.
- Berthelier, J. J., et al. (2006), ICE, the electric field experiment on DEMETER, *Planet. Space Sci.*, *54*, 456–471.
- Christian, H. J., et al. (2003), Global frequency and distribution of lightning as observed from space by the optical transient detector, *J. Geophys. Res.*, *108*(D1), doi:10.1029/2002JD002347.
- Clilverd, M. A., C. J. Rodger, R. Gamble, N. P. Meredith, M. Parrot, J. J. Berthelier, and N. R. Thomson (2008), Ground-based transmitter signals observed from space: Ducted or non-ducted?, *J. Geophys. Res.*, *113*(A04211), doi:10.1029/2007JA012602.
- Cummer, S. A. (2000), Modeling electromagnetic propagation in the earth-ionosphere waveguide, *IEEE Transactions on Antennas and Propagation*, *48*(9), 1420–1429.
- Fiser, J., J. Chum, G. Diendorfer, M. Parrot, and O. Santolík (2010), Whistler intensities above thunderstorms, *Ann. Geophys.*, *28*, 37–46.
- Gamble, R. J., C. J. Rodger, M. A. Clilverd, J.-A. Sauvaud, N. R. Thomson, S. L. Stewart, R. J. McCormick, M. Parrot, and J. J. Berthelier (2008), Radiation belt electron precipitation by man-made vlf transmitters, *J. Geophys. Res.*, *113*(A10211), doi:10.1029/2008JA013369.
- Gemelos, E. S., U. S. Inan, M. Walt, M. Parrot, and J. A. Sauvaud (2009), Seasonal dependence of energetic electron precipitation: Evidence for a global role of lightning, *Geophys. Res. Lett.*, *36*(L21107), doi:10.1029/2009GL040396.
- Green, J. L., S. Boardsen, L. Garcia, W. W. L. Taylor, S. F. Fung, and B. W. Reinisch (2005), On the origin of whistler mode radiation in the plasmasphere, *J. Geophys. Res.*, *110*(A03201),

doi:10.1029/2004JA010495.

- Gurnett, D. A., and U. S. Inan (1988), Plasma wave observations with the Dynamic Explorer 1 spacecraft, *Reviews of Geophysics*, *26*, 285–316.
- Gustafsson, G., N. E. Papitashvili, and V. O. Papitashvili (1992), A revised corrected geomagnetic coordinate system for epochs 1985 and 1990, *J. Atm. and Terr. Phys.*, *54*(11–12), 1609–1631.
- Koons, H. C., and J. L. Roeder (1990), A survey of equatorial magnetospheric wave activity between 5 and 8  $r_e$ , *Planet. Space Sci.*, *38*(10), 1335–1341.
- Meredith, N. P., R. B. Horne, M. A. Clilverd, D. Horsfall, R. M. Thorne, and R. R. Anderson (2006), Origins of plasmaspheric hiss, *J. Geophys. Res.*, *111*(A09217), doi: 10.1029/2006JA011707.
- Meredith, N. P., R. B. Horne, S. A. Glauert, and R. R. Anderson (2007), Slot region electron loss timescales due to plasmaspheric hiss and lightning-generated whistlers, *J. Geophys. Res.*, *112*(A08214), doi:10.1029/2007JA012413.
- Meredith, N. P., R. B. Horne, S. A. Glauert, D. N. Baker, S. G. Kanekal, and J. M. Albert (2009), Relativistic electron loss timescales in the slot region, *J. Geophys. Res.*, *114*(A03222), doi: 10.1029/2008JA013889.
- Němec, F., O. Santolík, M. Parrot, and J. Bortnik (2008), Power line harmonic radiation observed by satellite: Properties and propagation through the ionosphere, *J. Geophys. Res.*, *113*(A08317), doi:10.1029/2008JA013184.
- Parrot, M. (1990), World map of ELF/VLF emissions as observed by a low-orbiting satellite, *Ann. Geophys.*, *8*, 135–145.

- Parrot, M., U. Inan, N. Lehtinen, E. Blanc, and J. L. Pincçon (2008), HF signatures of powerful lightning recorded on demeter, *J. Geophys. Res.*, *113*(A11321), doi:10.1029/2008JA013323.
- Parrot, M., et al. (2006), The magnetic field experiment IMSC and its data processing onboard DEMETER: Scientific objectives, description and first results, *Planet. Space Sci.*, *54*, 441–455.
- Rodger, C. J., M. A. Clilverd, and R. J. McCormick (2003), Significance of lightning-generated whistlers to inner radiation belt electron lifetimes, *J. Geophys. Res.*, *108*(A12), doi:10.1029/2003JA009906.
- Rodger, C. J., R. J. McCormick, and M. A. Clilverd (2004), Testing the importance of precipitation loss mechanisms in the inner radiation belt, *Geophys. Res. Lett.*, *31*(L10803), doi:10.1029/2004GL019501.
- Rodger, C. J., M. A. Clilverd, and N. R. Thomson (2005), Lightning driven inner radiation belt energy deposition into the atmosphere: Regional and global estimates, *Ann. Geophys.*, *23*(11), 3419–3430.
- Santolík, O., M. Parrot, and J. Chum (2008), Propagation spectrograms of whistler-mode radiation from lightning, *IEEE Transactions on Plasma Science*, *36*(4), 1166–1167.
- Santolík, O., M. Parrot, U. S. Inan, D. Burešová, D. A. Gurnett, and J. Chum (2009), Propagation of unducted whistlers from their source lightning: A case study, *J. Geophys. Res.*, *114*(A03212), doi:10.1029/2008JA013776.
- Voss, H. D., M. Walt, W. L. Imhof, J. Mabilia, and U. S. Inan (1998), Satellite observations of lightning-induced electron precipitation, *J. Geophys. Res.*, *103*(A6), 11,725–11,744.
- Walker, A. D. M. (1993), *Plasma Waves in the Magnetosphere*, Springer-Verlag, Berlin, Germany.

**Figure 1.** Distribution of Magnetic Local Times (MLT) at which DEMETER took the measurements.

**Figure 2.** Maps in geomagnetic coordinates showing the day-time median value of power spectral density of electric field fluctuations in the frequency range 1–10 kHz for: (top) May-October (bottom) January-April and November-December.

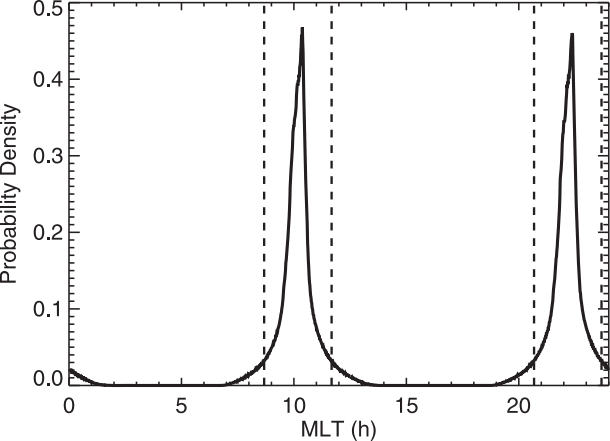
**Figure 3.** The same as Figure 2, but for the night-time.

**Figure 4.** (top) Geomagnetic map of lightning activity during the night-time for May-October. (middle) The same as in the top panel, but “symmetrized” by using the total lightning activity at the conjugate regions. (bottom) The same as in the middle panel, but projected along the magnetic field-lines up to the DEMETER altitude.

**Figure 5.** The same as Figure 4, but for January-April and November-December period.

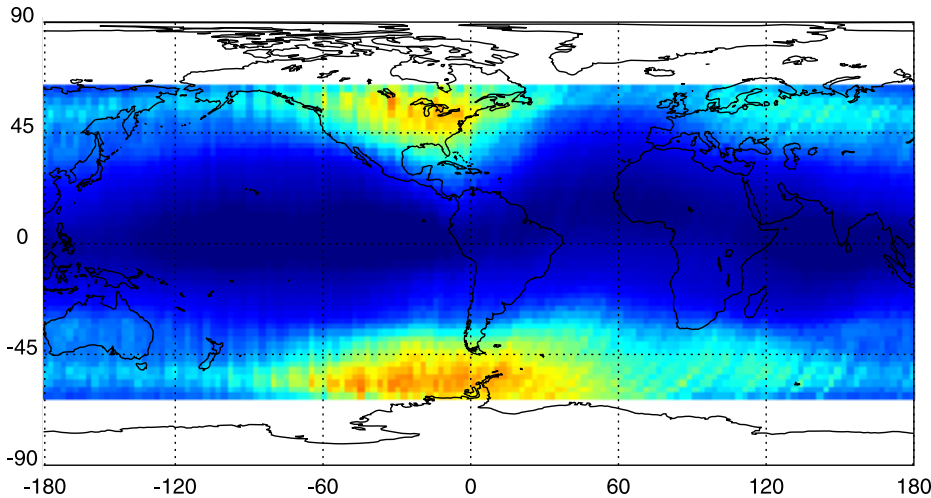
**Figure 6.** (top) Day-time median value of power spectral density of electric field fluctuations above the USA during May-October period as a function of frequency and absolute value of the geomagnetic latitude. A solid black line represents one half of the equatorial electron cyclotron frequency calculated at the given L-value using a dipole magnetic field model. (middle) The same as the top panel, but this time for January-April and November-December period. (bottom) Lightning occurrence rate as a function of the geomagnetic latitude during the day-time (red) and during the night-time (blue). Dashed lines trace the projections along the magnetic field lines up to the satellite altitude.

**Figure 7.** The same as Figure 6, but for the night-time.

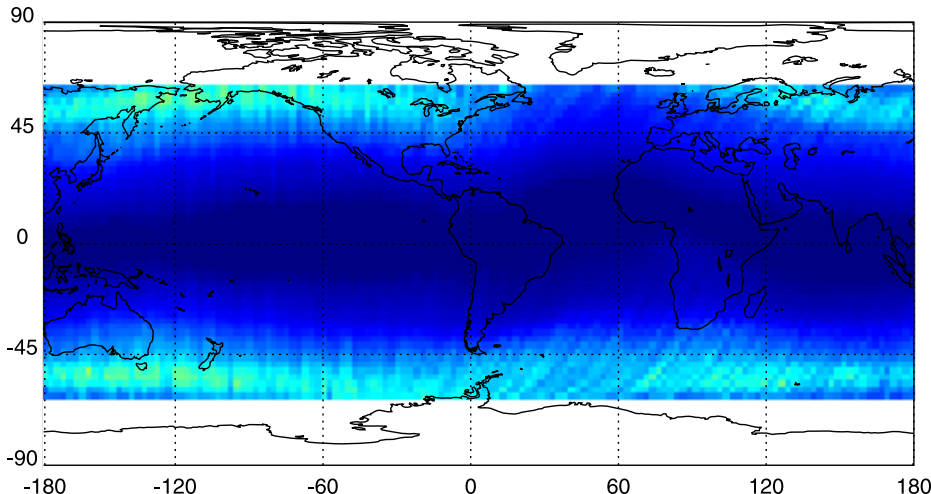


-3.0      -2.5      -2.0      -1.5      -1.0      -0.5      0.0  
 $\log(\mu\text{V}^2 \text{m}^{-2} \text{Hz}^{-1})$

May-October

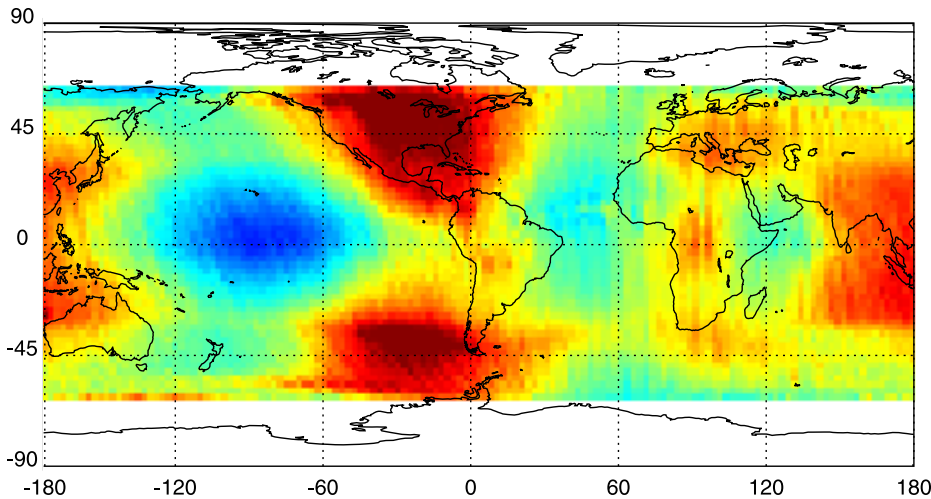


Jan-April, Nov-Dec

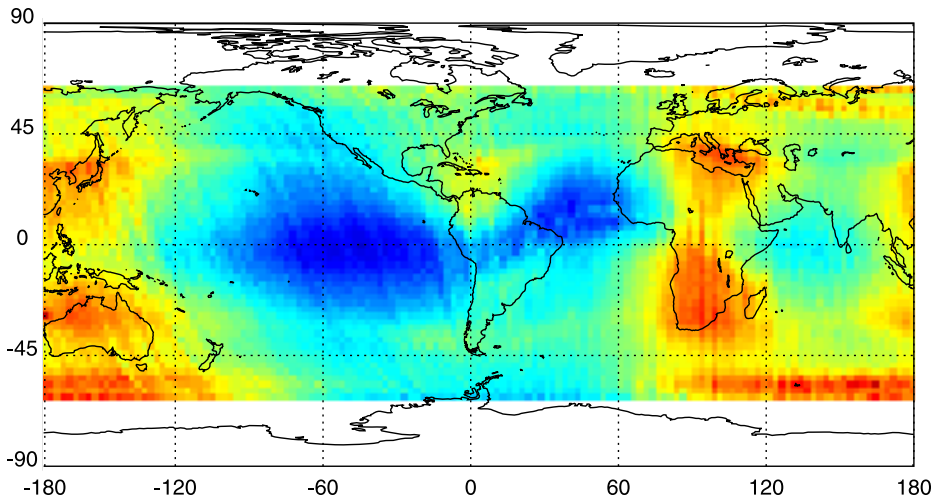


-3.0      -2.5      -2.0      -1.5      -1.0      -0.5      0.0  
 $\log(\mu\text{V}^2 \text{m}^{-2} \text{Hz}^{-1})$

May-October

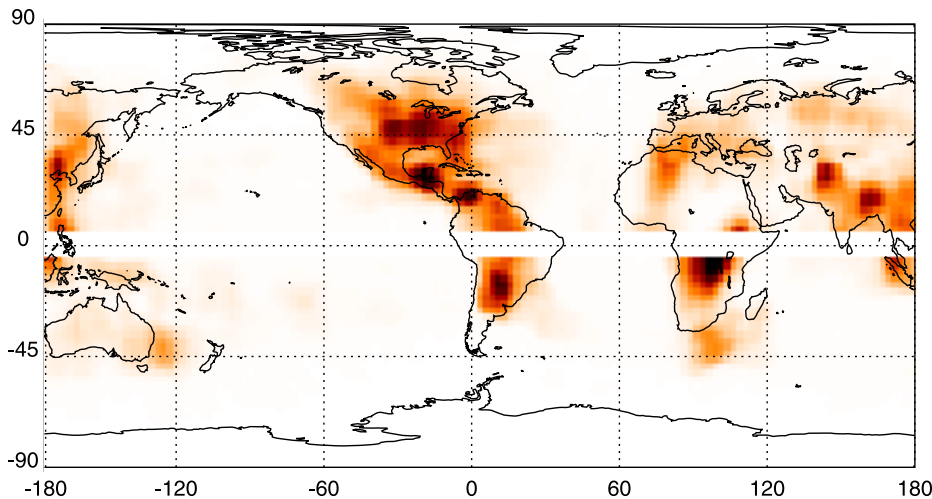


Jan-April, Nov-Dec

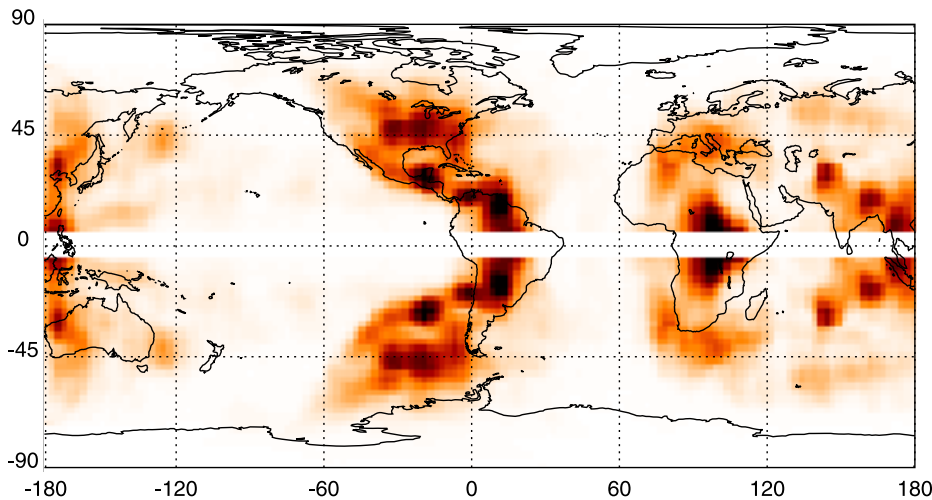


0.0 0.5 1.0 1.5 2.0 2.5 3.0  
Flashes  $\text{km}^{-2} \text{yr}^{-1}$

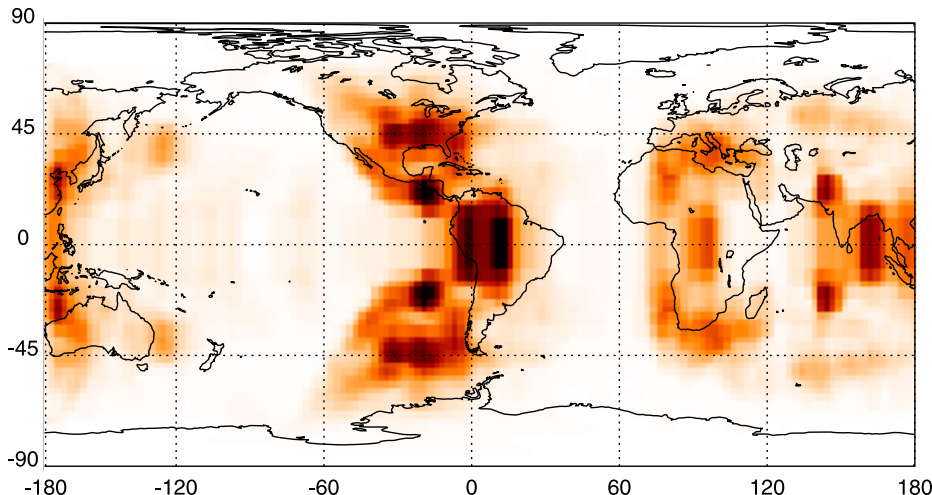
Original



Symmetrized

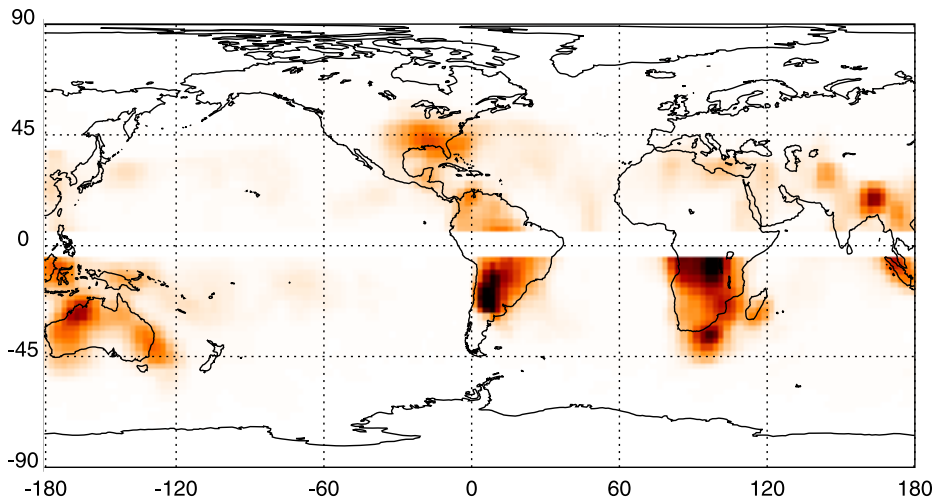


Field line projection

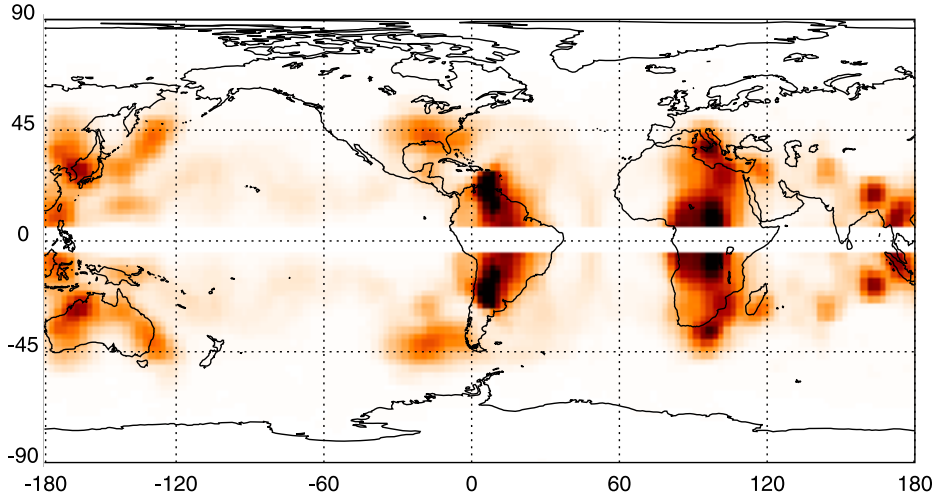


0.0 0.5 1.0 1.5 2.0 2.5 3.0  
Flashes  $\text{km}^{-2} \text{yr}^{-1}$

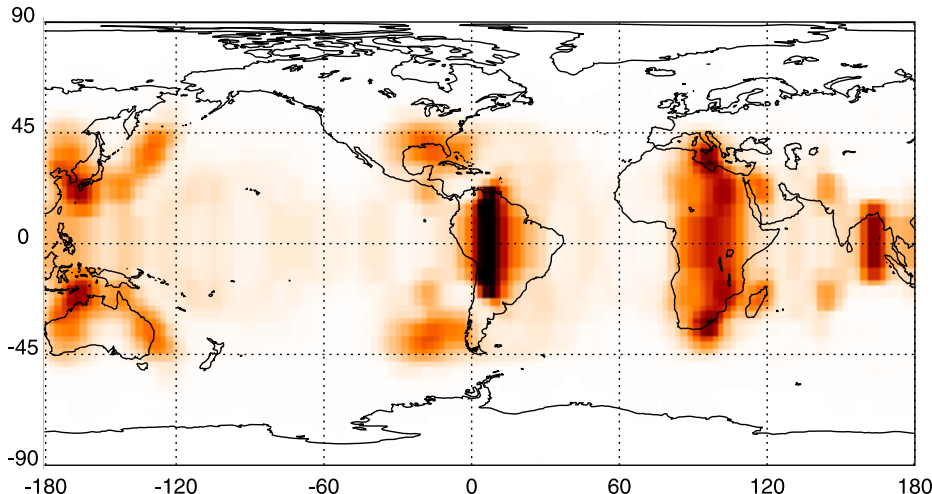
Original



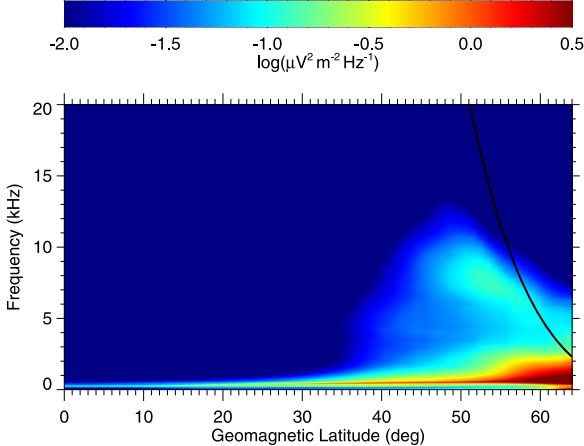
Symmetrized



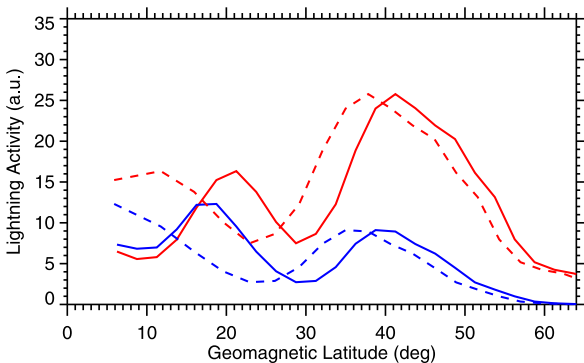
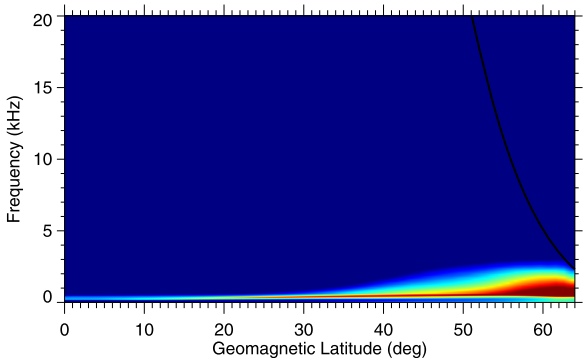
Field line projection



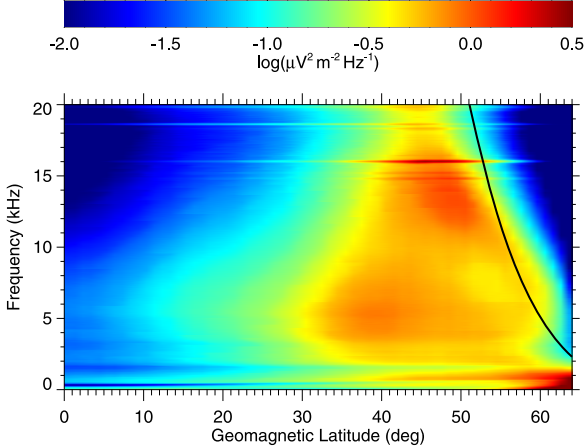
May-October



Jan-April, Nov-Dec



May-October



Jan-April, Nov-Dec

